



HAL
open science

Quasi thermal noise spectroscopy in the inner magnetosphere of Saturn with Cassini/RPWS: Electron temperatures and density

Michel Moncuquet, Alain Lecacheux, Nicole Meyer, Baptiste Cecconi, William S. Kurth

► **To cite this version:**

Michel Moncuquet, Alain Lecacheux, Nicole Meyer, Baptiste Cecconi, William S. Kurth. Quasi thermal noise spectroscopy in the inner magnetosphere of Saturn with Cassini/RPWS: Electron temperatures and density. *Geophysical Research Letters*, 2005, 32 (L20S02), pp.1-5. 10.1029/2005GL022508 . hal-03733063

HAL Id: hal-03733063

<https://hal.science/hal-03733063>

Submitted on 19 Aug 2022

HAL is a multi-disciplinary open access archive for the deposit and dissemination of scientific research documents, whether they are published or not. The documents may come from teaching and research institutions in France or abroad, or from public or private research centers.

L'archive ouverte pluridisciplinaire **HAL**, est destinée au dépôt et à la diffusion de documents scientifiques de niveau recherche, publiés ou non, émanant des établissements d'enseignement et de recherche français ou étrangers, des laboratoires publics ou privés.

Copyright

Quasi thermal noise spectroscopy in the inner magnetosphere of Saturn with Cassini/RPWS: Electron temperatures and density

Michel Moncuquet,¹ Alain Lecacheux,¹ Nicole Meyer-Vernet,¹ Baptiste Cecconi,^{1,2} and William S. Kurth²

Received 19 January 2005; revised 28 April 2005; accepted 18 May 2005; published 29 June 2005.

[1] On 1 July 2004, the Cassini spacecraft performed its Saturn orbit insertion, twice crossing the equatorial plane between the G and F rings. The radio HF receiver observed a peak at the upper-hybrid frequency and weakly banded emissions having well-defined minima at gyroharmonics. We show that through most of the encounter, these emissions do not result from instabilities, but instead are the quasi-thermal noise that can be calculated from the classical theory of plasma fluctuations. The spectroscopy of this noise yields the electron density, the core and the halo temperatures in the range $2.3 < L/R_S < 7$, $-1.2 < z/R_S < +0.1$. For the first time, we measure the core temperature of the Kronian plasma torus to be about 0.5 eV in the ring plane at $\sim 2.5R_S$, and increasing to ~ 6 eV at $7R_S$. From the noise minima at the gyroharmonics, we also deduce the magnetic field strength, which agrees with the Cassini's magnetometer data to better than 2%. **Citation:** Moncuquet, M., A. Lecacheux, N. Meyer-Vernet, B. Cecconi, and W. S. Kurth (2005), Quasi thermal noise spectroscopy in the inner magnetosphere of Saturn with Cassini/RPWS: Electron temperatures and density, *Geophys. Res. Lett.*, 32, L20S02, doi:10.1029/2005GL022508.

1. Introduction

[2] The first explorations of planetary magnetospheres showed that the spectral density measured with an electric antenna peaks at the upper hybrid frequency $f_{uh} = \sqrt{f_g^2 + f_p^2}$, where $f_g = \omega_g/2\pi$ is the electron gyrofrequency (or cyclotron frequency) and $f_p = \omega_p/2\pi$ is the plasma frequency. This was observed at Saturn for the first time by *Gurnett et al.* [1981] and *Pedersen et al.* [1981]. Figure 1 shows the dynamic spectrum acquired by the Radio and Plasma Wave Science High Frequency Receiver (RPWS-HFR) on the electric dipole antenna of Cassini (called X-dipole hereinafter) during the SOI (Saturn orbit insertion on 1 July 2004 with a closest approach near 03 UT). One can see the peak at f_{uh} that emerges from the background around 21 UT and becomes spectacular until ~ 01 , then “disappears” until ~ 04 where it strongly peaks again, to finally smoothly vanishes ~ 09 UT.

[3] In addition to the f_{uh} peak, we shall focus in the present paper on the Bernstein waves (that is, electrostatic

waves propagating quasi-perpendicularly to the magnetic field \mathbf{B} , noted BW herein) which peak (Figure 1) between the harmonics of the gyrofrequency f_g , while much less strongly than the peak at f_{uh} (except sporadically in the first gyroharmonic band), namely from ~ 2330 to 01 and from ~ 04 to 06 UT. The detection of these weakly banded emissions, which are minima at the gyroharmonics, will allow us to determine f_g as shown by the white continuous curve on Figure 1. We show in section 2 that we can provide much more than merely a “ f_{uh} or f_g diagnostic”, as we can also deduce the electron core and halo temperatures from the minima and maxima levels of the voltage power spectra. This is because in a large part of this Cassini-Saturn encounter, the spectral density measured is just the power spectrum of the fluctuations induced by the thermal motion (or quasi-thermal, if the velocity distribution is not a pure Maxwellian) of the ambient electrons and ions -the so-called quasi-thermal noise (QTN hereinafter). This noise can be quantitatively calculated from the particle velocity distribution using the theory of plasma fluctuations [*Sitenko*, 1967]. Our results on electron density, the core and the halo temperatures are summarized on Figure 2. In section 3, we briefly discuss the low temperature found in the inner plasma torus and the vertical scale height estimated from the electron density. We finally explain why the peak of noise at f_{uh} vanishes throughout the Cassini flyover of the main Saturn rings (i.e. Cassini closer than $2.3R_S$ to Saturn). All quantities read in SI units.

2. Measuring Plasma Parameters With the Electric Antennas of Cassini

[4] We consider frequencies sufficiently high that ion motions can be neglected and shall assume the electron velocity distribution $f(v)$ in the inner magnetosphere to be a sum of two Maxwellians (core + halo) of total density $N_e = N_c + N_h$ and temperatures T_c and T_h for the core and halo population respectively. The calculation of the QTN with such a core + halo distribution has been done by *Meyer-Vernet and Perche* [1989] for a non-magnetized plasma and extended to the magnetized case by taking into account the contribution of BW by *Sentman* [1982] and *Meyer-Vernet et al.* [1993] under the assumption that the plasma is stable. This assumption can be verified a posteriori by the relative smooth temporal variation and by the compatibility of the observed amplitudes with the QTN calculated with a moderate T_h . It is noteworthy that, for a non-magnetized plasma, most of the QTN comes from waves with wavelength greater than or close to the cold electron Debye length $L_D = \sqrt{k_B T_c / m_e \omega_p}$. For a magnetized plasma,

¹Laboratoire d'Etudes Spatiales et Instrumentation en Astrophysique, Observatoire de Paris, Paris, France.

²Department of Physics and Astronomy, University of Iowa, Iowa City, Iowa, USA.

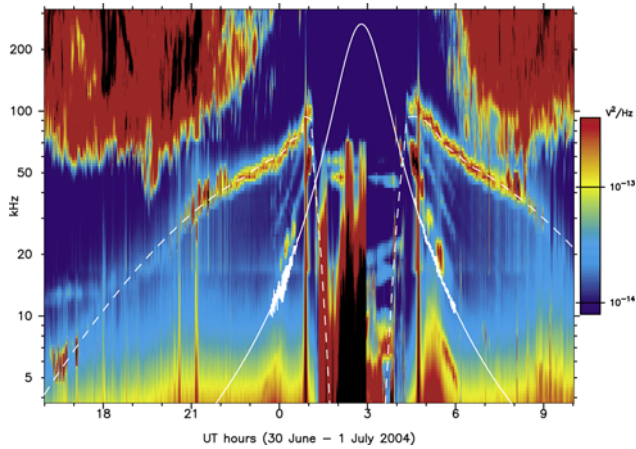


Figure 1. Radio spectrogram acquired on the X-axis dipole by the RPWS-HF receiver on Cassini during 18 hours of the closest approach day (30 June–1 July 2004). The white continuous line is the gyrofrequency f_g determined from Bernstein wave detection and extrapolated to the whole spectrogram from the best detection period (from ~ 05 to 06 UT). The white dashed line shows an empirical model of f_p extrapolated along the Cassini trajectory as explained in section 3.

additional QTN comes from BW with wavelengths close to the cold electron gyroradius $\rho_c = \sqrt{k_B T_c / m_e \omega_g}$ (this assertion is valid only for $\rho_c > L_D$).

[5] We claim that the noise is minimum at the gyroharmonics and that the enhancement between these gyroharmonics is produced by the halo of the electron velocity distribution. Let us briefly explain this point: a general condition for electrons of velocity \mathbf{v} to resonate with an electrostatic wave (\mathbf{k}, ω) in a magnetized plasma is $\omega - k_{\parallel} v_{\parallel} = n\omega_g$, where n is an integer. So “true” BW ($k_{\parallel} = 0$) are damped at gyroharmonics but propagate almost without damping between them. Small k_{\parallel} modes are excited between the gyroharmonics by the halo (because it requires large v_{\parallel}), and strongly damped at the gyroharmonics by the core. Thus they contribute to enhance the QTN only between the gyroharmonics.

2.1. f_g From the Minima at Gyroharmonics and Deducing N_e

[6] We first exploit the fact that the noise is minimum (below f_{uh}) at the harmonics of the gyrofrequency. The detection of these minima on both dipole and monopole antennas yields f_g with an accuracy of $\sim 2\%$ when compared to the MAG magnetometer experiment (see Figure 3). Then, from our best determination of f_g (which occurs during the ~ 0430 to 06 UT period), we have extrapolated the white curve plotted on Figure 1 (simply assuming a perfect non-tilted magnetic dipole for Saturn), which also matches the inbound measurements rather well. The latter are much noisier than outbound (this is mainly because BW cannot be detected on the Z-monopole during this period). From each spectrum where f_{uh} is detected, we deduced $f_p = \sqrt{f_{uh}^2 - f_g^2}$ and thus the electron density $N_e = \epsilon_0 m_e (2\pi/e)^2 f_p^2$. We have plotted N_e on Figure 2 as a black curve which annoyingly varies by steps due to the low spectral resolution (48 log-spaced channels from ~ 3 to 300 kHz) achieved during the

SOI. The insufficient spectral resolution unfortunately precludes further investigations such as estimation of the plasma bulk velocity (corotation) from the Doppler shift of the minima or as detection of f_Q resonances of BW just above f_{uh} [e.g., *Moncuquet et al.*, 1997], and makes superfluous a fitting of an accurate QTN model to the data.

2.2. T_c From the QTN Minimum Level

[7] If the receiver is quiet and sensitive enough (and it is), we expect that the minimum level of the spectral density V^2 is dominated (for the dipole antenna and below f_p) by the electron QTN. Because we have $f_g \ll f_p$ during the periods where f_{uh} is detected (i.e. time periods excluding ~ 01 to 04 UT), the computation of the QTN minimum is roughly equivalent to its computation in an unmagnetized plasma. This minimal level is given as a function of the core temperature T_c and local Debye length L_D by:

$$V_{\min}^2 \approx \frac{8\sqrt{2m_e k_B}}{\pi^{3/2} \epsilon_0} \sqrt{T_c} \int_0^{\infty} \frac{F(kL) k L_D^2}{[k^2 L_D^2 + 1]^2} dk \quad (1)$$

Here F is the response to electrostatic waves of the electric dipole on Cassini, which is a V-shaped wire antenna with each arm of length $L = 10$ m forming an angle $\Phi = 120^\circ$ [see *Meyer-Vernet and Perche*, 1989, equation 18 and section 6.1.2]. Note that for $L_D \ll L$, we can use $F(kL) \sim \pi/(4kL)$, and (1) reduces to: $V_{\min}^2 \approx 3 \times 10^{-13} T_c / (L f_p)$ (this roughly applies for $L_D \lesssim 1$ m, i.e. when Cassini was inside the Mimas orbit). Two provisos are in order before using (1) to determine T_c :

[8] 1. The spectral density, which is actually measured at the receiver inputs instead of the antenna terminals, has to

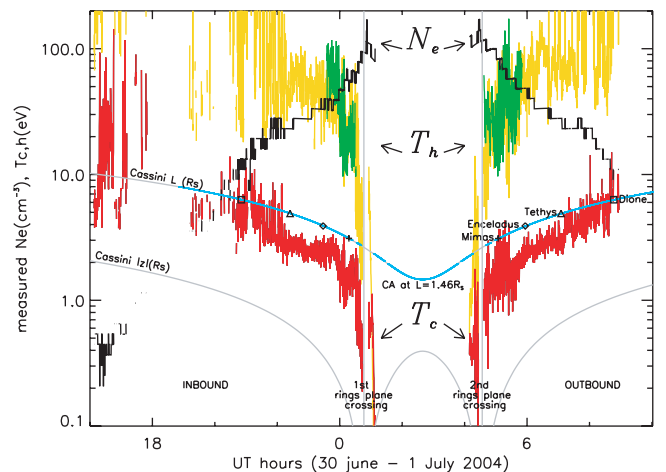


Figure 2. Electron parameters measured in the inner magnetosphere of Saturn with QTN spectroscopy. The electron density N_e is plotted in black and the core electron temperature T_c in red. The halo (hot) electron temperature T_h is plotted in yellow (when deduced from the f_{uh} peak) or superposed in green (when deduced from intraharmonic peaks). The grey curves show the altitude $|z|$ of Cassini over the equatorial plane and the L-shell of Cassini in the Saturn magnetic dipole (both read in Saturn radii R_S on the vertical log scale). Along the L curve, we have also indicated the L-shell of the main inner icy satellites (symbols) and of the E, G, F, A and B rings (in blue).

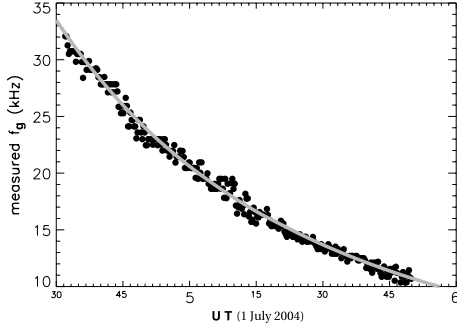


Figure 3. Comparison between f_g as deduced from QTN in Bernstein waves (dots) and from the MAG measurement (gray line).

be corrected by an attenuation factor due to the finite impedance of the pre-amplifier+receiver system which can be considered as a pure capacitance: $V_R^2(\omega) = V^2(\omega)/(1 + C_b/C_a)^2$ where C_a is the antenna capacitance and C_b the base capacitance of the antenna mounting structure. For the dipole, Zarka *et al.* [2004] have found $C_b \simeq 89$ pF and the antenna capacitance is theoretically given, for $\omega < \omega_p$, by: $C_a = \pi\epsilon_0 L/\ln(L_D/a)$, where $a \simeq 1.4$ cm is the wire radius.

[9] 2. Another contribution to the spectral density is due to the charged particles which impact the antenna and to the photoelectrons and secondary particles that it emits. Unfortunately and contrary to the QTN, the impact noise level may strongly depend on the S/C floating potential [see Meyer-Vernet and Perche, 1989]. For the dipole, and assuming that the floating potential is vanishingly small, this impact noise (also called “shot noise”) is:

$$V_i^2 = 2 \frac{\sqrt{2m_e k_B T_c}}{\pi^{3/2} \epsilon_0} A \left[\frac{f_p}{f} \right]^2 \approx 2 \cdot 10^{-16} A \sqrt{T_c} \left[\frac{f_p}{f} \right]^2 \quad (2)$$

with $A = a[\ln(L_D/a)]^2/L$ for $a \ll L_D < L$ and $A = a[\ln(L/a) - 1]^2/L (\approx 0.044)$ for $L_D > L$. Note that equation (2) underestimates the temperature when the S/C is charged negatively. But we may remark from (2) that the impact noise is dominant at LF and then decreases as f^{-2} . We have used this property which is verified on almost all the spectra, to extrapolate as f^{-2} the impact noise from the LF to the frequency of the minimum noise level. We obtained in most cases a negligible or small contribution (<10%) to this level. However, when the impact noise is of the order or larger than the QTN at the minimum level, we can no longer compute T_c from (1) and we use (2) instead. This occurs only from 16 to 18 UT (i.e. during the inbound pass from 10 to 9 R_S) where we find $\langle T_c \rangle \sim 20$ eV, with very large standard deviations (see Figure 2).

2.3. Spectral Maxima: Measuring T_h

[10] Let us now estimate the noise level at its peaks, that are roughly midway between each intraharmonic band and at f_{uh} : both these maxima levels are mainly dependent on the hot electron temperature and will allow two different determinations of T_h .

2.3.1. T_h From QTN in Bernstein Waves

[11] It is beyond the scope of this paper to detail the calculation of the QTN near the mid-gyroharmonic bands. Let us only summarize it by equation (3), which was used to

obtain T_h (green curve on Figure 2) on the two periods where the BW were detected: (from ~ 2330 to ~ 01 UT and from ~ 04 to ~ 06 UT)

$$V_{mid}^2 \simeq 2.6 \cdot 10^{-18} F_{\perp}^V(\eta L/2\rho_c) \left(T_h/\sqrt{T_c} \right) \quad (3)$$

$$\simeq 2.6 \cdot 10^{-18} (SL/\rho_c)^2 \left(T_h/\sqrt{T_c} \right), \text{ for } \rho_c > L/3 \quad (4)$$

$$\simeq 1.3 \cdot 10^{-14} T_h/(L f_g), \text{ for } \rho_c \ll L \quad (5)$$

Here F_{\perp}^V is the response of a V-shaped X-antenna (of V-angle Φ) to BW, $S = \sin \Phi/2$ and $\eta = \max(\cos \theta \cos \Phi/2, \sin \theta \sin \Phi/2)$ where θ is the angle between the Cassini X-axis and \mathbf{B} ($\eta \sim 0.5$ during almost all the studied periods -courtesy of the MAG team). The approximations (4) and (5) use the behavior of $F_{\perp}^V(u) \sim (Su)^2$ and $\sim 8/u$ for small and large u respectively. In practice, equation (4) shows that the signal enhancement between gyroharmonics will rapidly vanish for $\rho_c \gtrsim SL \approx 8.7$ m (this merely reflects the antenna sensitivity), that we have actually observed.

2.3.2. T_h From the QTN Maximum

[12] At $\sim f_{uh}$, the power spectrum exhibits a maximum which behaves much like the peak near f_p for isotropic plasma when $f_g \ll f_p$ [Meyer-Vernet and Perche, 1989]. This condition is verified in our data, except during the period from ~ 01 to 04 UT not studied here. With a core + halo distribution, the noise peak amplitude is mainly proportional to T_h/T_c and is given by the following expression, valid for $L_D \ll L$ [Meyer-Vernet and Perche, 1989, Table 4]:

$$V_{max}^2 \approx 0.036 (L/L_D)^2 (T_h/T_c) V_{min}^2 \quad (6)$$

Substituting (1) into (6) then yields V_{max}^2 from which we determine T_h . The result is plotted as the yellow curve in Figure 2. Let us note that the two independent T_h determinations agree rather well.

3. Discussion

3.1. Temperatures

[13] The core electron temperature is found as low as ~ 0.5 eV in the ring plane at $\sim 2.5 R_S$, to steeply increase up to ~ 1.5 eV at $2.8 R_S$ (the G-ring). Such a cold temperature was expected from the Voyager 1 and 2 surveys [Sittler *et al.*, 1983], but, to the best of our knowledge, was never measured (the particle analyzers had a threshold at 10 eV). Then T_c regularly increase from 1.5 eV up to $\sim 5-6$ eV near

Table 1. Equatorial Electron Density $N_e(0, L)$, Scale Height H and Deduced Ion Temperature T_i During Cassini’s Orbit Insertion.

L-shell (R_S)	7–4.5	4.5–3.4	3.4–2.3	2.3–1.46
z range (R_S)	[–1.2, –0.5]	[–0.5, –0.2]	[–0.2, 0.1]	[0.1, 0.4]
$N_e(0, L)$ (cm^{-3})	40–50 ^a	50–70 ^a	70–110 ^a	110
H (R_S)	0.9	0.7–0.6 ^a	0.35	0.1
T_i (eV)	20	12–10 ^a	3	0.25

^ainbound-outbound determinations, respectively.

the Dione L-shell ($6.3R_S$). The uncertainty in T_c is estimated from its standard deviation as about 25%. These results are in good agreement with the extended plasma model proposed by *Richardson* [1995, and references therein] and compatible with the 10 eV measured by *Voyager 1* at Dione's L-shell [*Sittler et al.*, 1983]. However, a clear discrepancy with the *Richardson's* model is the lower temperature of the hot population inside the Mimas L-shell ($3.1R_S$) which is found here to be ~ 20 – 30 eV (with $\sim 40\%$ uncertainty from the standard deviation), whereas it is ~ 70 – 80 eV in the model. Beyond the Mimas orbit, T_h increase strongly to ~ 60 eV, and up to ~ 100 eV beyond *Tethys*, but T_h is rather poorly determined there. Inversely, we may remark that T_h and T_c plummets when *Cassini* goes through the ring plane, both inbound and outbound; this could be due to a plasma cooling effect by the dust [see *Sittler et al.*, 1983, section 10.3.4]. Let us finally note that T_c is not provided for the two short periods of the ring plane traversal by *Cassini* (see Figure 2). This is because the spectral density is dominated by impacts of dust grains on the antenna body [*Meyer-Vernet et al.*, 1998]; such a study is beyond the scope of this paper.

3.2. Density

[14] The measured density has a maximum at 170 cm^{-3} in the equatorial plane (which is also the ring plane), and decreases on both sides with increasing altitude z of *Cassini*. The electron density is also in good agreement with the model of *Richardson* [1995]. In order to examine briefly the large scale structure of the plasma torus encountered by *Cassini*, we have fit to our density data a crude Gaussian model of confinement for a plasma assumed in perfect corotation with Saturn, neglecting any anisotropy or velocity filtration effects, whose centrifugal, magnetic and spin equators coincide. It simply reads: $N_e(z, L) = N_e(0, L) \exp[-z^2/H(L)^2]$, where $N_e(0, L)$ and $H(L)$ are approximated by step-like functions. The results of the fit are given in Table 1 (except from $2.3R_S$ to the CA -see last remark below). Note that the inbound density is $\sim 25\%$ lower than outbound. In the simple case where there is a single ion species of mass m_i with a temperature T_i much larger than T_e , we have approximately: $H \approx \sqrt{2k_B T_i / 3m_i \Omega_{spin}^2}$, where Ω_{spin} is Saturn's spin rate. We have also indicated in Table 1 the T_i computed from the fitted H , assuming a generic "water group" ion of 16 proton masses. Because this method yields parallel ion temperatures (since H depends on the parallel pressure), our ion temperature estimates are consistent with the perpendicular ion temperatures measured by *Voyager*, with a temperature anisotropy of $T_\perp/T_\parallel \approx 5$ for the heavy ions, as reported by *Richardson and Sittler* [1990]. Finally, the white dashed curve plotted on Figure 1 is the f_p deduced from the above empirical model, and gives an idea of the reasonable quality of the fit; it follows rather well the QTN peak when $f_{uh} \sim f_p$, and slightly separates from the peak when f_g increases (as long as $f_p > f_g$).

[15] This last remark brings us to a last result: while the decrease with distance of the peak amplitude at f_{uh} can be ascribed to the antenna response when $L_D \gtrsim L$, the sudden vanishing of the f_{uh} resonance at $\sim 2.3R_S$, both inbound and outbound, stems from the fact than f_p becomes lower than f_g (or equivalently $L_D > \rho_c$). Indeed in that case, there is no resonance (i.e. zero of the plasma dielectric function) at f_{uh} .

One of the extensions of this paper will be to develop the QTN analysis for this case. Nevertheless, we may claim that $f_p < f_g \approx 40 \text{ kHz}$ at $\sim 2.3R_S$, i.e. the density plummets from ~ 100 to 20 cm^{-3} at this distance. This can be explained by either a scale height drop-off (i.e. a very strong plasma cooling) or a true decrease in equatorial density, or likely both of these reasons. As an upper limit for cooling, we have assumed in Table 1 that $N_e(0, L)$ remains constant at 110 cm^{-3} , so that the scale height must decrease to $0.1 R_S$, i.e. T_i as low as 0.25 eV (the corresponding f_p is plotted as the steep dashed lines on Figure 1). Because this coincides with *Cassini's* flyby of the densest A and B rings, we suggest that the plasma inside $2.3R_S$ is strongly cooled and rarefied by interaction processes with the ring materials.

4. Conclusions

[16] From the interpretation of the spectral density measured with the *Cassini* electric antennas as Quasi-Thermal Noise (QTN), and thanks to a good knowledge/calibration of the RPWS antennas and HF-receiver, we have measured the electron density, the core and halo electron temperatures and the magnetic field strength in the inner magnetosphere of Saturn, that is mainly from the Dione L-shell (within the E-ring) to the A-ring external edge. In particular, we have measured for the first time the core electron temperature in the inner Kronian plasma torus, to be as low as 0.5 eV at the ring plane crossings (at $\sim 2.5R_S$). This is one of the strong points of QTN spectroscopy to allow the measurement of such a low electron temperature using only a sensitive and well calibrated radio receiver.

[17] Let us finally emphasize that the spectral density measured on 1 July 2004 with the *Cassini* antennas was qualitatively and quantitatively the "QTN in Bernstein modes" that we could expect, adapting the method we have successfully performed [*Meyer-Vernet et al.*, 1993; *Moncuquet et al.*, 1995, 1997] on the spectra acquired by *Ulysses* on 8 February 1992 in the Io plasma torus, although with rather different antennas in a hotter and denser plasma. From a pure 'space physics' point of view, it is noteworthy that the Bernstein waves, often called "n + 1/2" cyclotron emissions, which are ubiquitous in planetary magnetospheres, are generally not produced by instabilities but are in most cases steady quasi-thermal emissions sustained by the suprathermal electron population.

[18] **Acknowledgments.** *Cassini*-RPWS activities at LESIA are supported by the French CNES (Centre National d'Études Spatiales). The University of Iowa is supported by NASA through contract 961152 with the Jet Propulsion Laboratory.

References

- Gurnett, D. A., W. S. Kurth, and F. L. Scarf (1981), Plasma waves near Saturn—Initial results from *Voyager 1*, *Science*, *212*, 235–239.
- Meyer-Vernet, N., and C. Perche (1989), Tool kit for antennae and thermal noise near the plasma frequency, *J. Geophys. Res.*, *94*, 2405–2415.
- Meyer-Vernet, N., S. Hoang, and M. Moncuquet (1993), Bernstein waves in the Io plasma torus: A novel kind of electron temperature sensor, *J. Geophys. Res.*, *98*, 21,163–21,176.
- Meyer-Vernet, N., A. Lecacheux, and B. Pedersen (1998), Constraints on Saturn's G ring from the *Voyager 2* Radio Astronomy Instrument, *Icarus*, *132*, 311–320.
- Moncuquet, M., N. Meyer-Vernet, and S. Hoang (1995), Dispersion of electrostatic waves in the Io plasma torus and derived electron temperature, *J. Geophys. Res.*, *100*, 21,697–21,708.

- Moncuquet, M., N. Meyer-Vernet, S. Hoang, R. J. Forsyth, and P. Canu (1997), Detection of Bernstein wave forbidden bands in the Jovian magnetosphere: A new way to measure the electron density, *J. Geophys. Res.*, *102*, 2373–2380.
- Pedersen, B. M., M. G. Aubier, and J. K. Alexander (1981), Low-frequency plasma waves near Saturn, *Nature*, *292*, 714–716.
- Richardson, J. D. (1995), An extended plasma model for Saturn, *Geophys. Res. Lett.*, *22*, 1177–1180.
- Richardson, J. D., and E. C. Sittler (1990), A plasma density model for Saturn based on Voyager observations, *J. Geophys. Res.*, *95*, 12,019–12,031.
- Sentman, D. D. (1982), Thermal fluctuations and the diffuse electrostatic emissions, *J. Geophys. Res.*, *87*, 1455–1472.
- Sitenko, A. G. (1967), *Electromagnetic Fluctuations in Plasma*, Elsevier, New York.
- Sittler, E. C., K. W. Ogilvie, and J. D. Scudder (1983), Survey of low-energy plasma electrons in Saturn's magnetosphere: Voyagers 1 and 2, *J. Geophys. Res.*, *88*, 8847–8870.
- Zarka, P., B. Cecconi, and W. S. Kurth (2004), Jupiter's low-frequency radio spectrum from Cassini/Radio and Plasma Waves Science (RPWS) absolute flux density measurements, *J. Geophys. Res.*, *109*, A09S15, doi:10.1029/2003JA010260.
-
- B. Cecconi, A. Lecacheux, N. Meyer-Vernet, and M. Moncuquet, Laboratoire d'Etudes Spatiales et Instrumentation en Astrophysique, Observatoire de Paris, 5 Place Jules Janssen, Meudon F-92195, France. (michel.moncuquet@obspm.fr)
- W. S. Kurth, Department of Physics and Astronomy, University of Iowa, Iowa City, IA 52242, USA.